Synthesis and characterization of silica-coated oil-in-water (O/W) magnetic emulsion

Eslam Elkalla, Sumera Khizar, Zouhair Ait-Touchente, Noureddine Lebaz, Marie Hangouët, Guy Raffin, Nadia Zine, Abdelhamid Elaissari

Synthesis and Characterization of Silica-Coated Magnetic Oil-in-Water (O/W) Magnetic Emulsion

Eslam Elkalla [1], Sumera Khizar [1*], Zouhair Ait-Touchente [1,2], Noureddine Lebaz [2], Marie Hangouët [1], Guy Raffin [1], Nadia Zine [1] and Abdelhamid Elaissari [1,]

[1] Univ Lyon, University Claude Bernard Lyon-1, CNRS, ISA-UMR 5280, 69100 Villeurbanne, France

[2] Univ Lyon, University Claude Bernard Lyon-1, CNRS, LAGEPP UMR-5007, 69100 Villeurbanne, France

*Corresponding author. ISA, University Claude Bernard Lyon-1, 5 rue de la Doua, Villeurbanne 69100, France. Email address: sumera.khizar@univ-lyon1.fr

Graphical abstract:

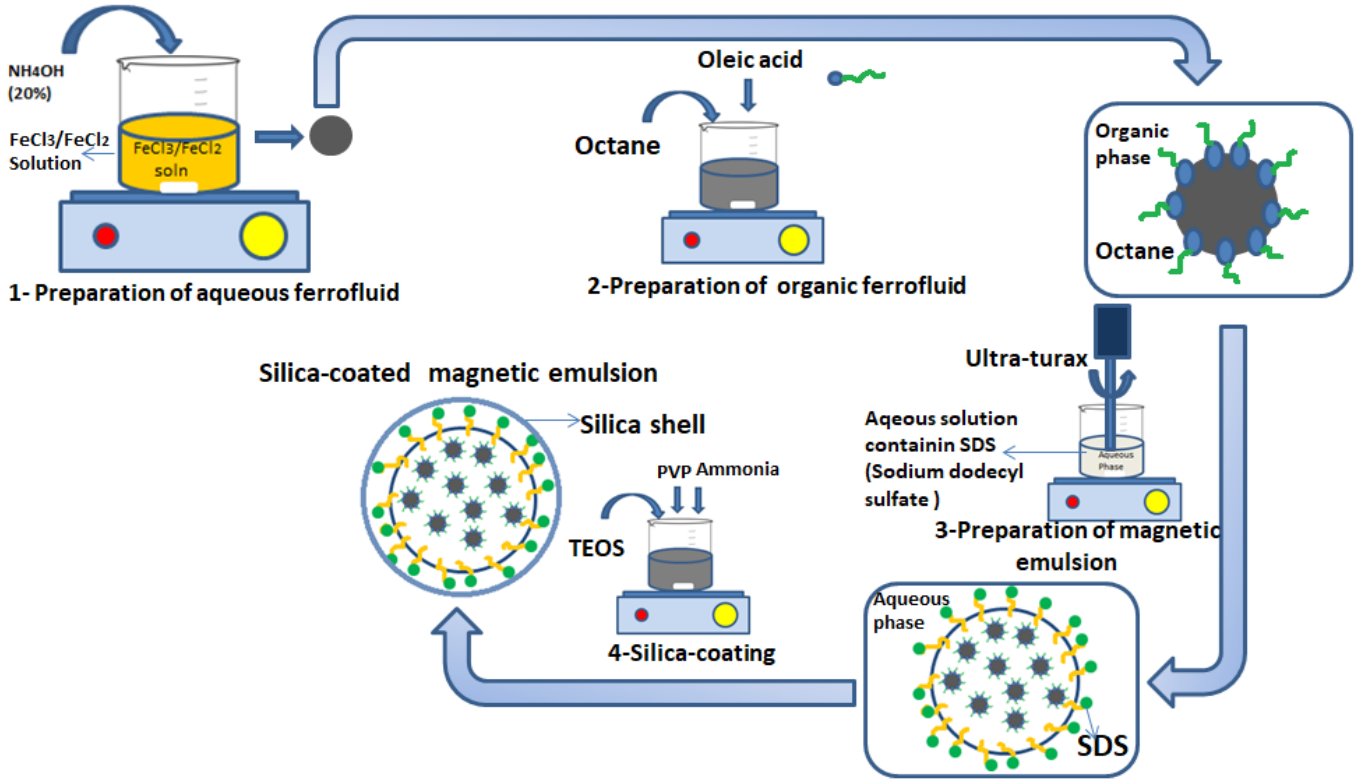

Abstract:

A stable emulsion of organic ferrofluid in an aqueous medium, known as oil-in-water (O/W) ferrofluid emulsion, was successfully prepared and characterized. The present study introduces a novel approach to synthesize and emulsify ferrofluid, followed by silica coating of the resulting nanoparticles using sol-gel process. The ferrofluid consisted of magnetic nanoparticles stabilized with oleic acid in octane. Both the ferrofluid and the emulsion exhibited spherical morphology, with average sizes of 20 nm and 200 nm, respectively. Characterization methodologies for instance TEM (transmission electron microscopy), DLS (dynamic light scattering), XRD, FTIR, and magnetic measurements were employed to determine the size distribution, crystallinity, morphology, and chemical composition of the nanoparticles. Chemical composition analysis of the prepared nanoparticles was performed using thermogravimetric analysis. This research work demonstrates the possibility of encapsulating O/W magnetic emulsion, promising potential for future bioapplications, emphasizing the importance of efficient and stable O/W ferrofluid emulsions.

Keywords: Oil-in-water emulsion. Organic ferrofluid. Magnetic nanoparticles. Silica shell.

1. Introduction:

The research on ferrofluids has significantly improved in last 50 years leading to a substantial extent of scientific knowledge and practical applications of these specific materials. These are artificial materials in which magnetism is present in a liquid state with high magnetic susceptibility [1]. Ferrofluids are acknowledged as nanoscale materials, serving as colloidal suspensions that consist of minute magnetic particles dispersed within aqueous or organic liquids. They exhibit interesting physiochemical characteristics (thermal, optical, magnetic, rheological, apparent density, etc.) under a magnetic stimulus have been at the forefront of research [2]. The presence of these magnetic properties enables effective control and manipulation of ferrofluids through the application of magnetic fields. Various approaches have been employed to synthesize ferrofluids, including hydrothermal technique, sol-gel pyrolysis, mechanochemical synthesis, flame synthesis, mechanical alloying, thermal decomposition, mechanical milling, coprecipitation, sonochemical method, and one-pot synthesis. [3]. Among all, well reported synthetic methods are coprecipitation and thermal decomposition, principally because of their ease and reliability [4,5]. Furthermore, these techniques provide more consistent results, require less equipment, and to best our knowledge are simply more thoroughly documented compared to other methods [6]. The applications of magnetic nanoparticles in diverse disciplines are growing day by day. There are countless reported applications of magnetic nanoparticles, counting medical imaging, biosensing, medicinal therapy, magnetic impedance, and magnetic nanoemulsions. Additional applications include energy harvesting and transfer, water treatment, and vibration control [7].

Typically, magnetic emulsions have three components: iron oxide nanoparticles, dispersion medium or carrier liquid and a surfactant to prevent their aggregation and to weaken magnetic interactions among them. But depending on the desired magnetic properties and applications, magnetic emulsions can consist of nanoparticles composed of mixed oxides containing cobalt, manganese, barium or nickel. Mostly maghemite (Fe_2O_3) and magnetite (Fe_3O_4) are employed for the synthesis of ferrofluids [8]. The stability regarding emulsions not only depends on the affinity between surfactant and carrier liquid, but it also depends on the method of synthesis and size of the nanoparticles. Ferrofluid emulsions have gained significant recognition due to their distinct properties, such as cytocompatibility, affinity to biological systems, nanoscale dimensions, superparamagnetic behavior, and swift magnetic field responsiveness[9]. Consequently, they have found diverse applications spanning from the field of biomedicine to bioengineering sectors [10]. In the biomedical domain, ferrofluid emulsions find significant utility as carriers for drug delivery, contrast agents, antimicrobial agents, as well as heat mediators in hyperthermia [11]. Additionally, their applications extend to biosensors, including magnetic impedance biosensors. The use of magnetic emulsions in biomedical diagnosis is because of superparamagnetic properties of magnetic nanoparticles. Its first application in biomedical diagnosis was in immunoassay. The second use was developed in nucleic acid based diagnostics: specific capture and non-specific capture, purification and concentration of nucleic acid material (DNA and RNA). Another application is related to cell sorting in vivo or in vitro [12].

One of the challenges of utilizing magnetic nanoparticles is their tendency to aggregate due to their high surface energy and strong magnetic attraction potential [13]. To address this issue, surface modification techniques such as coating with silica shells have been developed. Silica coating provides a protective shell around the magnetic core, which can prevent aggregation and enhance biocompatibility of nanoparticles [14]. Stöber Sol-gel method is the simplest route for silica coating that offers a functional interface for attaching biomolecules such as proteins, peptides, and antibodies. This enables precise transportation of magnetic nanoparticles to particular cells or tissues, providing targeted delivery. Silica-coated magnetite nanoparticles (SMNP) recently gained much attraction in biomedical, environmental, construction and nuclear

applications. Extensive research has focused on their investigation in treatment applications such as drug delivery, neutron capture therapy (NCT), hyperthermia, imaging applications for instance magnetic resonance imaging (MRI), magnetic particle imaging (MPI) and computed tomography (CT), and separation and detection applications for nucleic acids, cells, and proteins [15]. They exhibit excellent properties, high biocompatibility, chemical and thermal stability, and ease of functionalization. Moreover, silica protects magnetic nanoparticles against acid leaching and aggregation as well as increases their physiochemical stability and cytocompatibility [16]. Previous investigations reported that silica-based magnetic nanoparticles also present several biological proprieties, for instance antitumor, anti-protozoal, antibacterial, and stroke treatment [17]. Liquid capsules can also be formulated using Sol-gel method to contain precise amounts of active ingredients, which can be particularly important for medications with narrow therapeutic windows or where precise dosing is critical [18]. This can help to ensure that patients receive the correct dose of medication, which can improve treatment outcomes and reduce the risk of side effects [14].

Considering the significance and distinctive characteristics of ferrofluids, the present study aims to prepare oil-in-water (O/W) magnetic emulsion through the emulsification process involving organic ferrofluid in an aqueous medium. The organic ferrofluid was synthesized via coprecipitation method and stabilized in octane. Subsequently, this magnetic fluid was emulsified in an aqueous surfactant solution to achieve a stable emulsion consisting of magnetic colloidal particles. To enhance their stability, the magnetic nanoparticles were subjected to a silica coating using sol-gel process. Various analytical techniques were employed to assess the properties of the prepared ferrofluid, the resulting emulsion, and the silica-coated magnetic nanoparticles [19,20]. The research work described here is novel and elaborate the encapsulation of SDS stabilized organic ferrofluid by silica shell to form liquid capsules and solid shell. The synthesis of stable emulsion involving combination of organic ferrofluid with SDS is significant from several perspectives. This strategy provides a new, simple, economical, environmentally friendly, efficient, and likely scalable route to encapsulate organic ferrofluid inside silica shell efficiently without evaporation of octane and involvement of the complicated carrier design. The developed silica-coated magnetic particles could be promising efficient diagnostic bioapplications in future.

2. Materials and Methods

2.1. Materials

$FeCl_2.4H_2O$, $FeCl_3.6H_2O$, HCl (35%), NH_3 (25%), oleic acid, ethanol 96%, polyvinylpyrrolidone (PVP), tetraethyl orthosilicate (TEOS), and analytical-grade octane were obtained from Sigma-Aldrich (Germany). Sodium dodecyl sulfate (SDS), an anionic surfactant, was also acquired from Sigma-Aldrich (Germany). Ultra-pure water was employed in the formulation of all solutions. All chemicals and materials were of analytical grades and used as received.

2.2. Methods

2.2.1. Aqueous ferrofluid preparation

The coprecipitation technique is commonly employed for synthesizing ferrofluids by reducing metallic elements using various salt conditions [21]. To initiate the synthesis, ferrous chloride (3.7 g) and ferric chloride (10.16 g) were dissolved in 80 ml of ultrapure water. Once the iron salts completely dissolved, resulting in a homogeneous orange solution, 80 ml of concentrated ammonia solution (25%) was swiftly introduced into 50 ml thermostated round-bottom four necked flask reactor, equipped with a glass anchor-shaped stirrer, condenser, and nitrogen inlet (same reactor which is used for batch emulsion polymerization reactions) while vigorously stirring at 500 rpm. The immediate formation of a dark precipitate indicated the generation of iron oxide.

2.2.2. Organic ferrofluid preparation

The aqueous ferrofluid mentioned above was placed in above-mentioned reactor and subjected to gentle stirring. Following one hour, 8 ml of oleic acid was gradually introduced with stirring at a speed of 500 rpm. After a two-hour interval, octane was incrementally added to the solution using a pipette and stirred for duration of 15 minutes. The mixture was left undisturbed overnight. During this time, the iron oxide nanoparticles coated with oleic acid spontaneously migrated from the ammoniac phase to the organic phase, resulting in a distinct separation between a transparent lower phase (aqueous) and an upper phase containing the ferrofluid organic component [22,23].

2.2.3. Preparation of magnetic oil-in-water (O/W) emulsion

To obtain the pre-emulsion, the gradual addition of the organic ferrofluid into an aqueous surfactant solution was carried out under moderate stirring conditions. The organic ferrofluid, which had been prepared beforehand, was dispersed within the SDS solution and subjected to intense shearing using an Ultra-Turrax device. Numerous samples were prepared through emulsification of prepared organic ferrofluid with aqueous solution containing SDS as an anionic surfactant. Various concentrations of SDS have been investigated to formulate the stable emulsion ranging from 2 to 16 wt%. The stirring speed (9500 rpm) and time (5 minutes) were kept constant. The emulsion mixture was then subjected to emulsification using an Ultra-Turrax device and subsequently filtered through glass wool.

2.2.4. Synthesis of silica-coated magnetic nanoparticles (Si-MN)

In this study, a sol-gel method was employed to coat magnetic emulsion with silica. Trimethoxysilane (TEOS) was utilized as the silica precursor, while 25% ammonia (NH_3) acted as the catalyst. To begin, 10 ml of magnetic emulsion was subjected to a wash with deionized water and then dispersed in a solution containing 3 ml of 10% PVP [22]. The resulting solution underwent agitation for duration of three hours. Subsequently, 5 ml of ammonia was introduced and further agitation was carried out for 15 minutes. Following this, different amount of TEOS with 1 ml of ethanol were added to the solution, which was then left under stirring overnight. The aim was to determine the optimal amount of TEOS for achieving the best silica shell coating of magnetic core. The silica-coated particles were subsequently separated using a magnet, washed with deionized water, and filtered through glass wool. The initial dispersion of the organic ferrofluid took place in octane, resulting in the formation of a stable colloidal solution. This dispersion played a crucial role in the subsequent stages of the synthesis process, allowing for a comprehensive investigation of the Si-MN core/shell structure while influenced by octane as the dispersing medium [24].

2.3. Characterization techniques

The average hydrodynamic diameter (D_h) and particle size distribution of the organic ferrofluid, emulsion, and silica-coated magnetic nanoparticles were determined using the Malvern Zetasizer (Nano ZS, Malvern Instruments Limited, U.K). The measurements were conducted in a 1 mM NaCl solution at 25 °C. The physical dimensions of the prepared magnetic nanoparticles were examined by employing Transmission Electron Microscopy (TEM, Netherlands) with a Philips CM120 microscope at the "Centre Technologique des Microstructures" (CT) at the University of Lyon (Villeurbanne, France). Samples for TEM analysis were prepared by dispersing 10 µL of sample in 900 µL of water (aqueous ferrofluid and silica-coated magnetic nanoparticles) and octane (organic ferrofluid), then dropped on grid and dried before analysis. The magnetic properties of the dried magnetic colloids were investigated at room temperature using a vibrating sample magnetometer (Automatic Bench of Magnetic Measurements-ABMM, U.K.) at the Claude Bernard University Lyon-1, Villeurbanne, France. X-ray diffraction (XRD) analysis was performed to determine the crystallinity of the prepared

nanoparticles using XRD diffractometer (Burker D8 advance). Fourier transform infrared (FTIR) analysis was carried out to study and identify chemical functional groups in the synthesized compound with a FTIR spectrometer –Nexus (Thermo-Fisher Nicolet) in the range of 400-4000 cm^{-1}. Thermogravimetric analysis of the organic ferrofluid and colloids was carried out using the thermogravimetric analyzer (TA Instruments Q50 series) under an inert atmosphere, with the temperature ranging from room temperature to 1000 °C at a heating rate of 10 °C/min.

3. Results and Discussions

It was found that the most stable emulsion was formulated by using 12 wt% SDS solution. Different samples were prepared by varying the concentration of SDS solution added to organic ferrofluid (solid content of 15 % wt/v) keeping the total volume (12 ml) of magnetic emulsion constant (Table 1). Figure 1 showed different images of oil in water magnetic emulsion prepared by emulsification process. It can be clearly observed from Figure 1, that EK1 is the most stable emulsion since no phases separation is observed. Other samples showed phase separation and sedimentation that revealed their instability. Subsequently, the most stable magnetic emulsion (EK1) was further characterized.

Table 1: Preparation of magnetic emulsions using different amounts SDS.

Sample	Organic Ferrofluid	SDS(12 wt%)	Observation
EK1	2ml	10ml	More stable
EK2	3ml	9ml	Not stable
EK3	4ml	8ml	Little Sedimentation
EK4	5ml	7ml	Phase separation and sedimentation
EK5	6ml	6ml	Sedimentation

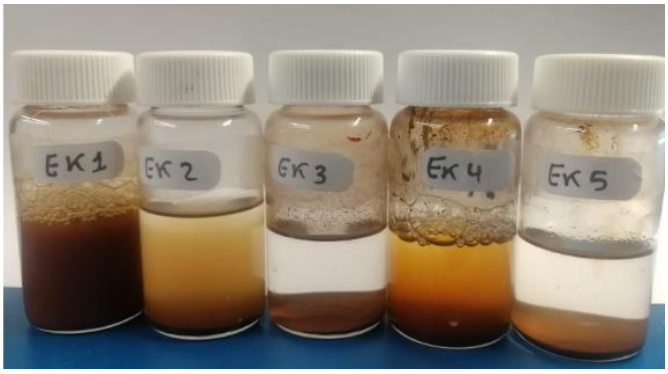

Figure 1. Different samples of emulsion prepared by emulsification of organic ferrofluid in SDS aqueous medium. **Please change the labeling (should not be by hand)**

3.1. Analysis of Aqueous Ferrofluid, Organic Ferrofluid, and Magnetic Emulsion Using Dynamic Light Scattering (DLS) and TEM

The hydrodynamic diameter (D_h) of the ferrofluid nanoparticles was measured to be 25 nm with an average value obtained from measurements carried out three times represented by three different colors (Figure 2a) [25]. ~~The findings indicate that the nanoparticles exhibited characteristics indicative of superparamagnetism.~~ Additionally, the polydispersity index (PDI) was determined and yielded a value of 0.482 (PDI = D_w/D_n) that indicates slight polydispersity in size of nanoparticles with a standard deviation (SD) of 13.69 nm. Figure 2b shows the TEM image of ferrofluid nanoparticles. TEM results showed that they have a nearly spherical shape and are uniformly distributed in size. The observed large particle size from DLS

compared to TEM analysis can be attributed to the presence of aggregated nanoparticles. This aggregation phenomena can be induced by low colloidal stability of the nanoparticles or attributed to ~~The agglomeration in such nanoparticles indicates~~ the influence of dipolar and magnetic interactions between the particles and has been frequently reported by literature [26,27]. These results showed that there are both single as well as multidomain magnetic nanoparticles [28].

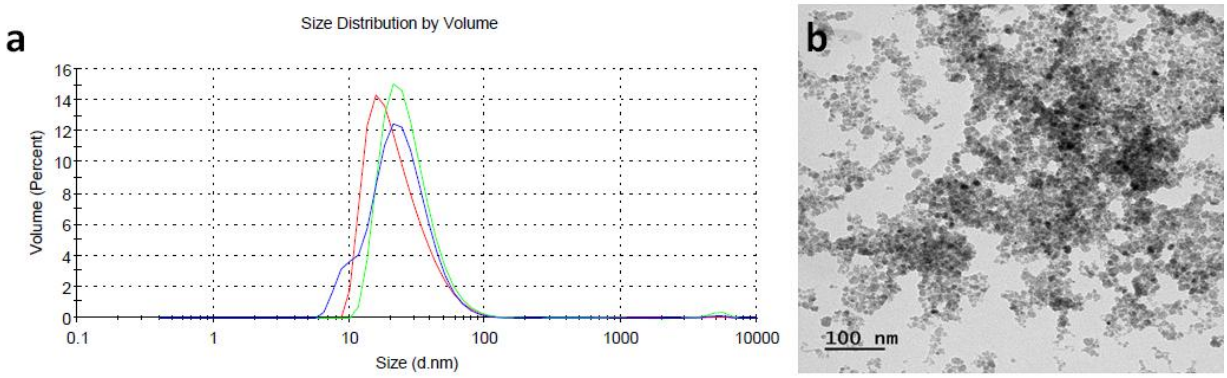

Figure 2. (a) Dynamic light scattering (DLS) analysis performed three times shown by three different colors and (b) TEM image of highly diluted aqueous ferrofluid.

The average size distribution of an organic ferrofluid showed an average size of 20 nm obtained from three measurements as shown in Figure 3a. This showed that particles possess nanoscale dimensions with PDI of 0.419 and standard deviation (SD) was calculated to be 10.39 nm. TEM image of organic ferrofluid particles (Figure 3b) indicated an average particle size of less than 50 nm. The magnetic particles appeared to be nearly spherical in shape. Results indicated that nanoparticles stabilized in octane showed minimum aggregation that promotes homogeneous distribution [29,30] .

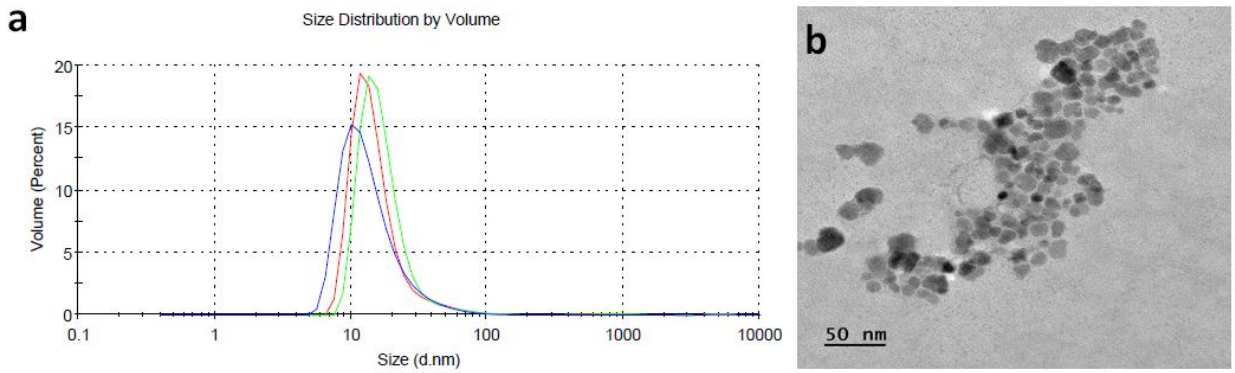

Figure 3. (a) Dynamic light scattering (DLS) analysis performed three times shown by three different colors and (b) TEM image of highly diluted organic ferrofluid (in octane).

~~Figure 4 gives~~ The size distribution of the most stable emulsion (EK1 in Table 1) is reported in Figure 4. The mean droplet size is around 200 nm. This value was determined by averaging the results of three separate measurements. The PDI value of 0.209 with a standard deviation of 92.28 nm suggests a nearly monodisperse system with excellent colloidal stability as macrospically demonstrated above. The hydrodynamic particle size distribution offers insights into emulsion stability, considering the concentration and type of surfactant used, as well as experimental conditions. However, further studies are required to optimize the emulsion preparation process and ensure consistent hydrodynamic particle size distribution. Obtaining a TEM image of the magnetic emulsion is challenging due to the presence of octane within the emulsion [31].

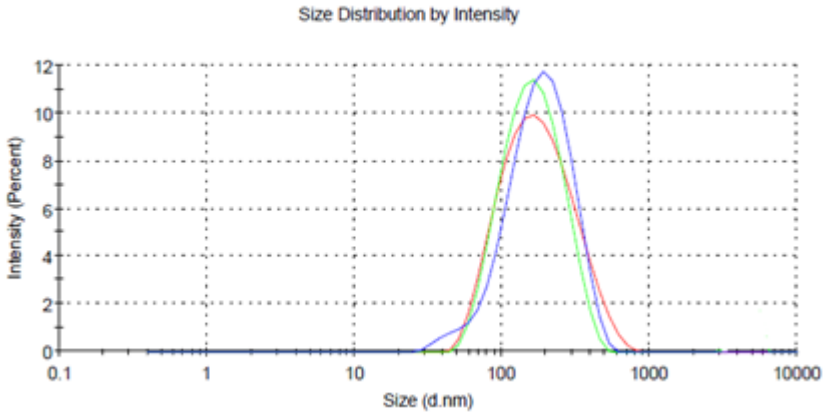

Figure 4. Dynamic light scattering (DLS) analysis of EK1 performed three times shown by three different colors.

Figure 5 (a, b, c and d) displays TEM images from various experiments carried out with different amounts of TEOS (50 µL, 100 µL, 150 µL, 200 µL) consecutively, revealing the presence of magnetic particles and silica particles surrounding the magnetic core. However, it is evident from TEM images that clear core-shell morphology has not been achieved [32] and only secondary nucleation (free silica nanoparticles) are produced and no any uniform silica shell is observed.

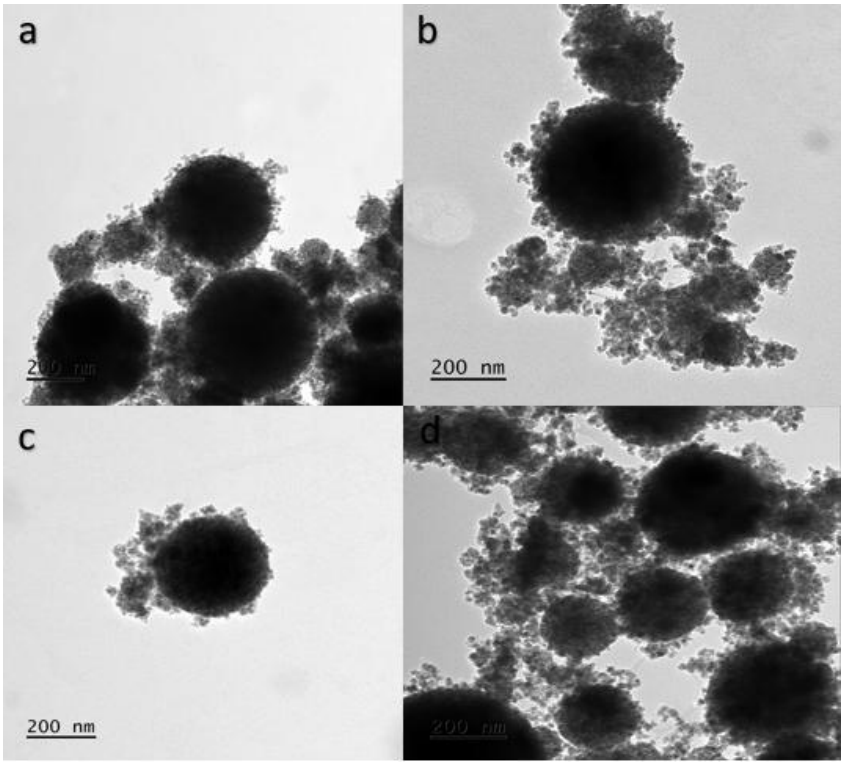

Figure 5. TEM image of Si-MN core/shell nanoparticles. (a) 50 µL, (b) 100 µL, (c) 150 µL, and (d) 200 µL.

The most colloidally stable magnetic dispersion sample was with attained with 1.25 ml TEOS. The hydrodynamic size distribution analysis of these nanoparticles was performed in water ~~dispersion~~. These resulting particles comprise magnetic nanoparticles dispersed in octane are coated with a silica shell. The experimental findings displayed a predominant peak average size of 1 µm, as illustrated in Figure 6a. Moreover, Figure 6b exhibits TEM images of the obtained final particles, revealing the presence of a distinct silica shell enveloping the magnetic core. The thickness of the silica shell varied in the range of 9 nm to 19 nm, depending on the quantity of TEOS employed during the coating process. The TEM image

distinctly depicts individual Si-MN core/shell nanoparticles, with well-defined core and shell regions [33]. The core, comprised of magnetic nanoparticles, appears as a dark region, while the silica shell exhibits a lighter color. ~~Additionally, the TEM image captures the presence of the octane solvent, either as a surrounding medium or as residual droplets.~~ This TEM analysis facilitates the observation of the morphology and integrity of the Si-MN core/shell nanoparticles, which significantly influences their performance in various applications. The TEM image of the Si-MN core/shell nanoparticles ~~in the presence of octane serves~~ as a visual confirmation of the successful synthesis of these particles and lays the groundwork for further comprehensive analysis and characterization. Results for silica shell using TEOS are in good agreement with the previously reported literature [34,35]

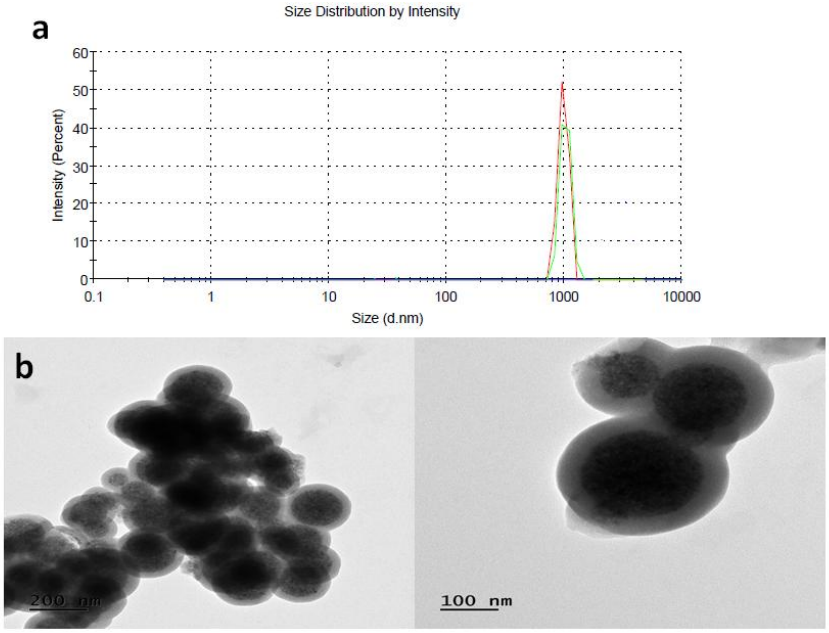

Figure 6. (a) Dynamic light scattering (DLS) analysis and (b) TEM image of Si-MN core/shell nanoparticles with 1.25 ml TEOS.

3.2. Magnetization of aqueous ferrofluid, organic ferrofluid, and O/W magnetic emulsion

The saturation magnetization of the magnetic emulsion, as depicted in Figure 7, was determined by extrapolating the magnetization ~~curve~~ versus ~~(M = f(1/H)) to~~ magnetic field curve ~~strength approaching infinity~~. Both the aqueous and organic ferrofluids exhibited magnetization values of approximately 80 emu/g and 75 emu/g, respectively, which closely resemble the bulk magnetite value of 92 emu/g [36]. This similarity suggests a robust magnetic response in both ferrofluids. Furthermore, the M-H curve in Figure 6 demonstrated a nearly linear increase in magnetization with the applied magnetic field, a characteristic commonly associated with superparamagnetic materials. The superparamagnetic behavior observed in the ferrofluids is attributed to the small size of the iron oxide nanoparticles, which contributes to their exceptional magnetic properties, including remanence [37]. However, it is worth noting that the magnetization of the organic ferrofluid was slightly lower than that of the aqueous ferrofluid, potentially due to the presence of magnetically inactive oleic acid [38]. Additionally, the magnetization of the magnetic emulsion was determined to be 40 emu/g, which is lower than the magnetization values of both the aqueous and organic ferrofluids. This decrease is attributed to the presence of non-magnetic components, such as oleic acid and sodium dodecyl sulfate (SDS), within the emulsion. It is important to consider that the magnetization values are influenced by various factors, including particle size, chemical composition ~~morphology~~, and crystal structure [39]. ~~Furthermore, the drying process during emulsion preparation can result in particle aggregation,~~

~~ultimately impacting the magnetic properties of the nanoparticles.~~ Despite the lower magnetization exhibited by the emulsion, it displays promising potential in several biomedical applications, including invitro biomedical diagnosis, sample preparation, drug delivery, magnetic hyperthermia, and magnetic resonance imaging [40].

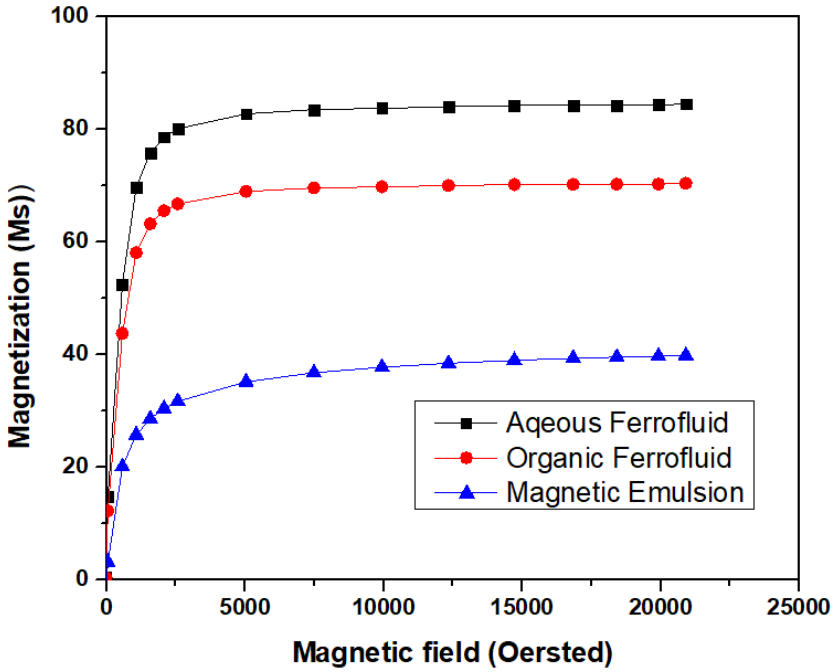

Figure 7. Magnetization versus magnetic field strength. (what is the unit of magnetization (emu/g) should be added) Ms should be changed by emu/g as used in the text

3.3. XRD analysis

The prepared nanoparticles were characterized by XRD for structural determination. The X-ray diffraction patterns of the organic ferrofluid is presented in Figure 8 that contains a series of characteristic peaks at 2 θ= 23.0°, 27.2°, 32.8°, 35.7o, 46.9°, 52.9°, 58.3°, 63.0°, and 78.0° are indexed as the diffractions of (111), (220), (311), (222), (331), (422), (511), (440), and (444) crystalline planes. The analysis of the diffraction pattern showed the formation of a cubic spinel structure in the sample, due to the strongest reflection that proceeds from the (311) plane that is in good accordance with the inverse cubic spinel phase of Fe3O4 (magnetite, Ref-code 01-075-1609). These results confirmed the crystalline structure of obtained magnetite nanoparticles, agreed with the structure of an inverse spinel-type oxide as reported in the literature [41,42]. Diffraction patterns of magnetic emulsion showed intense peaks at are 2θ = 6.78°, 20.0°, 21.7°, 22.6°, and 32.2° corresponding to the miller indexes (200), (213), (400), and (122), (311) respectively [43]. The XRD pattern of magnetic emulsion showed peak at 32.2° that corresponds to magnetite nanoparticles but of very low intensity. The new peaks correspond to SDS characteristics peaks [44,45]. The XRD pattern of silica-coated o/w magnetic particles displayed diffraction peaks at 6.89°, 11.3°, 13.5°, 31.7°, refer to (002), (200), (111), and (311) planes, respectively. The additional peak at 6.89° degree corresponds to SiO_2 [46,47]. This peak shows the presence of silica shell encapsulating magnetic o/w emulsion nanodroplets. The reduced intensity of (311) crystalline plane in emulsion and Si-MN is due to random crystal growth in which grains are not oriented correctly to allow diffraction to occur [48].

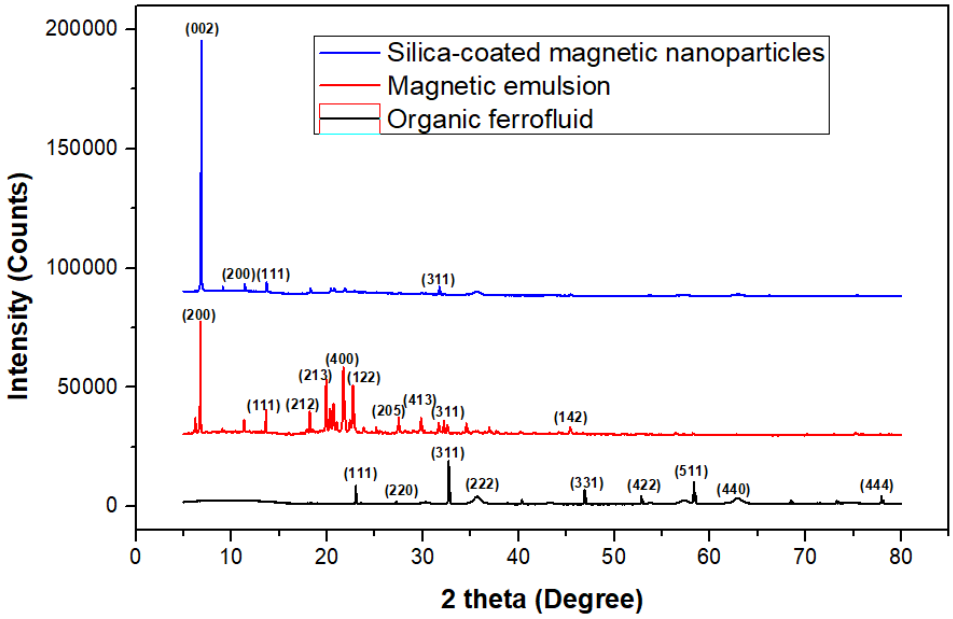

Figure 8. Comparison of XRD patterns of organic ferrofluid, magnetic emulsion, and silica-coated magnetic emulsion.
Should be use in the graph above

3.4. FTIR analysis of magnetic emulsion and silica-coated o/w magnetic emulsion

The FTIR spectra in Figure 9 depict the magnetic emulsion (ME) and silica-coated magnetic particles (Si-MN). Notably, an additional peak at 1220 cm^{-1} corresponds to the sulfate asymmetric stretch vibration, while two peaks at 1083 and 834 cm^{-1} relate to the sulfate symmetric stretch vibration [49]. These findings conclusively validate the existence of SDS within the magnetic emulsion samples. Distinctive bands characteristic of SDS molecules in the ME samples are absent in Si-MN. Instead, Two new peaks emerge at 1092 and 809 cm^{-1}, indicative of the presence of SiO_2 within the sample [50,51].

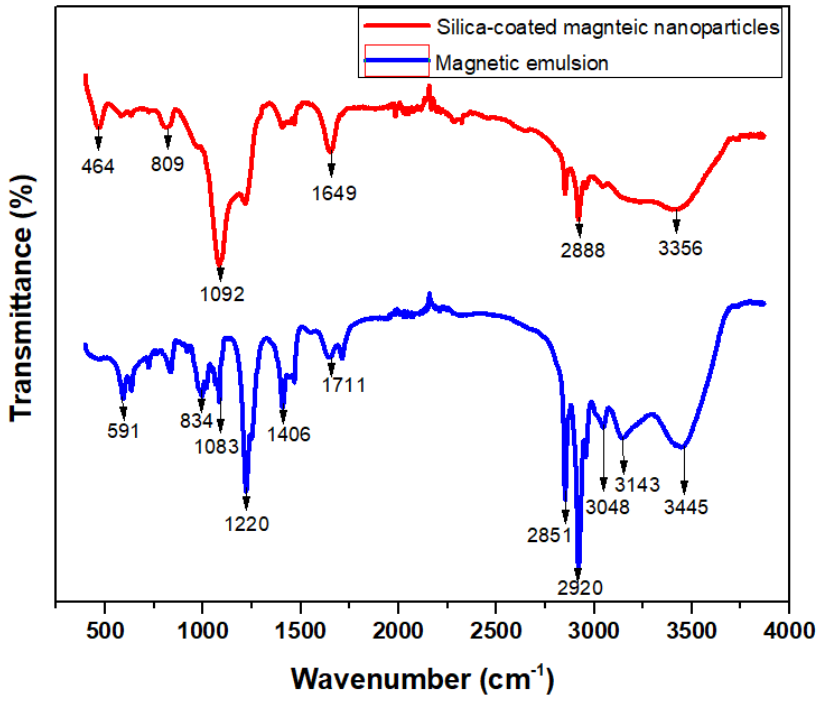

Figure 9. FTIR analysis of o/w magnetic emulsion and silica-coated o/w magnetic emulsion**.**

Please change silica-coated magnetic nanoparticles by silica-coated o/w magnetic emulsion in the figure

3.5. Thermogravimetric analysis of magnetic emulsion and silica-coated magnetic nanoparticles

The primary objective of conducting thermogravimetric analysis (TGA) was to assess the thermal behavior and chemical composition of the organic ferrofluid through the process of thermal decomposition. The TGA was carried out under an inert atmosphere, from room temperature to 1000 °C; with a heating rate of 10 °C/min. Figure 10 illustrates the TGA curve of the prepared magnetic emulsion which displayed two-step degradation, since an excess of oleic acid was utilized, resulting in free molecules of oleic acid predominantly orienting towards the water interface. The initial weight loss at 200 °C, is due to the desorption of the physically adsorbed water and the dehydroxylation of hydroxyl groups on the surface of magnetic nanoparticles. The degradation of oleic acid in organic ferrofluid is the cause of second weight loss above 200 °C. [13]. There was no significant thermal variation observed in these investigations. TGA of the magnetic emulsion demonstrated a gradual decrease in mass. Consequently, TGA analysis revealed that the magnetic emulsion comprised approximately 35% iron oxides and 65% oleic acid, which remained bounded to the nanoparticles [52].

TGA curve of Si-MN nanoparticles provided insights into the onset and rate of weight loss, revealing the presence of different components within the nanoparticles and their respective thermal decomposition behavior. As shown in Figure 7, the results indicated an overall weight loss of around 80.6% between 25 °C and 1000 °C, primarily attributed to the degradation of organic and volatile components present in the sample. The weight loss observed during TGA analysis could be divided into distinct steps. Initially, there was a weight loss of approximately 5.2% below 300°C associated with the degradation of TEOS and SDS at 120-140°C and 240°C, respectively. The degradation of oleic acid in Si-MN nanoparticles takes place between 250-300 °C [53]. PVP degrades at temperature between 400-450 °C [54]. Finally, a weight loss above 700°C is due to the phase transition of magnetic nanoparticles (from magnetite to hematite) [55]. Overall, there was a cumulative weight loss of 80%. Based on the mass loss data, the magnetic content within the Si-MN nanoparticles was estimated to be approximately 20%. The results showed that Si-MN nanoparticles are more stable than magnetic emulsion. A comprehensive understanding of the weight loss pattern and the contribution of different components enables a better comprehension of the chemical composition and thermal characteristics of the sample, thereby facilitating optimization of its synthesis and exploration of potential applications [13,55].

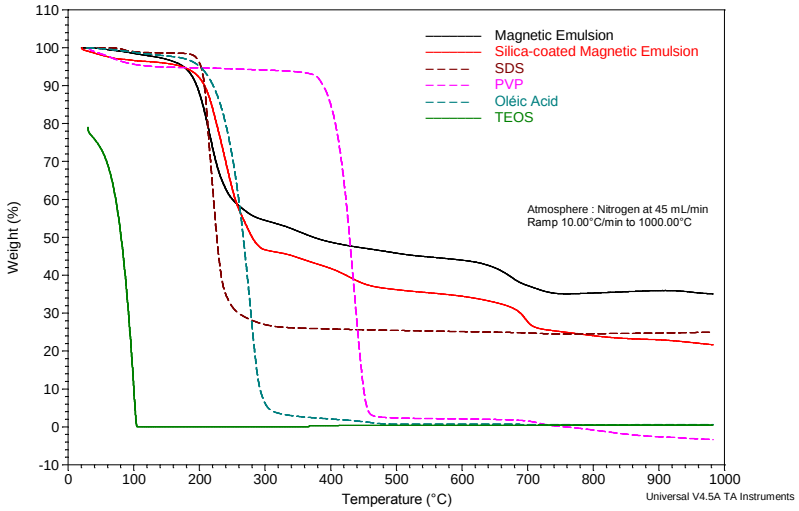

Figure 10. Thermal analysis of the prepared magnetic emulsion and silica-coated magnetic nanoparticles using thermogravimetric analysis (TGA).

4. Conclusions

The present work is focused on emulsification of organic ferrofluid and afterwards encapsulation of prepared magnetic o/w emulsion in silica shell. The simplest method of coprecipitation was employed to synthesize aqueous and organic ferrofluids. Organic ferrofluid was emulsified by single emulsion to formulate o/w magnetic emulsion consuming SDS as a surfactant. The prepared o/w magnetic emulsion ~~nanoparticles~~ were coated by silica shell by Sol-gel process. The size distribution of an aqueous and organic ferrofluid showed an average size of 25 and 20 nm, respectively. The mean o/w magnetic emulsion droplet size is around 200 nm ~~of magnetic emulsion~~, determined by dynamic light scattering analysis. TEM images indicated that the thickness of silica shell around ~~magnetic nanoparticles~~ o/w magnetic submicron droplet varies from 9 nm to 19 nm, depending on the quantity of TEOS employed during synthesis. The saturation magnetization of aqueous and organic ferrofluid was 80 and 75 emu/g, respectively which was higher than its colloidal solution which was found to be 40 emu/g due to surface modification. XRD analysis showed characteristic peaks of magnetite, SDS, and SiO_2. FTIR spectra showed characteristic bands of SDS molecules and SiO_2 that showed encapsulation of magnetic nanoparticles inside silica shell. The iron oxide contents were measured by TGA and found to be 35 and 20 % in the magnetic emulsion and silica-coated magnetic nanoparticles. Overall, this investigation establishes a solid foundation for future studies on silica-coated magnetic nanoparticles and their potential applications in the realms of biomedicine and environment.

Acknowledgements

Authors acknowledge the support of the ISA for support of present work.

Authors Contribution

Eslam Elkalla carried out experimental work and drafted a manuscript. Abdelhamid Elaissari designed and coordinated this research as a principal investigator. Sumera Khizar and Zouhair Ait-Touchente assisted in doing experiments and drafting manuscript. Noureddine Lebaz, Marie Hangouet, and Guy Raffin helped out in doing characterization. All other authors read and approved the final manuscript.

Data availability

The experimental data used to support the findings of this study are available from the corresponding author upon request.

Funding

This project received no external funding.

Declaration

The authors declare that there are no conflicts of interest regarding the publication of this paper.

References

1. W. FENNEI. Rosensweig, R. **1984**, 279.
2. Philip, J. Magnetic Nanofluids (Ferrofluids): Recent Advances, Applications, Challenges, and Future Directions. *Adv. Colloid Interface Sci.* **2023**, *311*, 102810, doi:10.1016/j.cis.2022.102810.
3. Kole, M.; Khandekar, S. Engineering Applications of Ferrofluids: A Review. *J. Magn. Magn. Mater.* **2021**, *537*, 168222, doi:10.1016/j.jmmm.2021.168222.
4. Vuong, T.K.O.; Tran, D.L.; Le, T.L.; Pham, D.V.; Pham, H.N.; Ngo, T.H. Le; Do, H.M.; Nguyen, X.P. Synthesis of High-Magnetization and Monodisperse Fe3O4 Nanoparticles via Thermal Decomposition. *Mater. Chem. Phys.* **2015**, *163*, 537–544, doi:10.1016/j.matchemphys.2015.08.010.
5. Maity, D.; Agrawal, D.C. Synthesis of Iron Oxide Nanoparticles under Oxidizing Environment and Their Stabilization in Aqueous and Non-Aqueous Media. *J. Magn. Magn. Mater.* **2007**, *308*, 46–55, doi:10.1016/j.jmmm.2006.05.001.
6. Paquin, F.; Rivnay, J.; Salleo, A.; Stingelin, N.; Silva, C. Multi-Phase Semicrystalline Microstructures Drive Exciton Dissociation in Neat Plastic Semiconductors. *J. Mater. Chem. C* **2015**, *3*, 10715–10722, doi:10.1039/b000000x.
7. Oehlsen, O.; Cervantes-Ramírez, S.I.; Cervantes-Avilés, P.; Medina-Velo, I.A. Approaches on Ferrofluid Synthesis and Applications: Current Status and Future Perspectives. *ACS Omega* **2022**, *7*, 3134–3150, doi:10.1021/acsomega.1c05631.
8. Wu, W.; Wu, Z.; Yu, T.; Jiang, C.; Kim, W.S. Recent Progress on Magnetic Iron Oxide Nanoparticles: Synthesis, Surface Functional Strategies and Biomedical Applications. *Sci. Technol. Adv. Mater.* **2015**, *16*, doi:10.1088/1468-6996/16/2/023501.
9. Ait-Touchente, Z.; Zine, N.; Jaffrezic-Renault, N.; Errachid, A.; Lebaz, N.; Fessi, H.; Elaissari, A. Exploring the Versatility of Microemulsions in Cutaneous Drug Delivery: Opportunities and Challenges. *Nanomaterials* **2023**, *13*, 1–19, doi:10.3390/nano13101688.
10. Zhang, Y.; Chan, H.F.; Leong, K.W. Advanced Materials and Processing for Drug Delivery: The Past and the Future. *Adv. Drug Deliv. Rev.* **2013**, *65*, 104–120, doi:10.1016/j.addr.2012.10.003.
11. Khizar, S.; Ahmad, N.M.; Ahmed, N.; Manzoor, S.; Elaissari, A. Encapsulation of Doxorubicin in Magnetic-Polymer Hybrid Colloidal Particles of Eudragit E100 and Their Hyperthermia and Drug Release Studies. *Polym. Adv. Technol.* **2020**, *31*, 1732–1743, doi:10.1002/pat.4900.
12. Kritika, N.; Roy, I. Therapeutic Applications of Magnetic Nanoparticles: Recent Advances. *Mater. Adv.* **2022**, *3*, 7425–7444, doi:10.1039/d2ma00444e.
13. Khizar, S.; Ahmad, N.M.; Saleem, H.; Hamayun, M.A.; Manzoor, S.; Lebaz, N.; Elaissari, A. Magnetic Colloidal Particles in Combinatorial Thin-Film Gradients for Magnetic Resonance Imaging and Hyperthermia. *Adv. Polym. Technol.* **2020**, *2020*, doi:10.1155/2020/7163985.
14. Fookes, F.A.; Mengatto, L.N.; Rigalli, A.; Luna, J.A. Controlled Fluoride Release for Osteoporosis Treatment

Using Orally Administered Chitosan Hydrogels. *J. Drug Deliv. Sci. Technol.* **2019**, *51*, 268–275, doi:10.1016/j.jddst.2019.03.004.

15. Mokkarat, A.; Kruanetr, S.; Sakee, U. One-Step Continuous Flow Synthesis of Aminopropyl Silica-Coated Magnetite Nanoparticles. *J. Saudi Chem. Soc.* **2022**, *26*, 101506, doi:10.1016/j.jscs.2022.101506.
16. Bruckmann, F. da S.; Nunes, F.B.; Salles, T. da R.; Franco, C.; Cadoná, F.C.; Bohn Rhoden, C.R. Biological Applications of Silica-Based Nanoparticles. *Magnetochemistry* **2022**, *8*, doi:10.3390/magnetochemistry8100131.
17. Ding, B.; Shao, S.; Xiao, H.; Sun, C.; Cai, X.; Jiang, F.; Zhao, X.; Ma, P.; Lin, J. MnFe2O4-Decorated Large-Pore Mesoporous Silica-Coated Upconversion Nanoparticles for near-Infrared Light-Induced and O2 Self-Sufficient Photodynamic Therapy. *Nanoscale* **2019**, *11*, 14654–14667, doi:10.1039/c9nr04858h.
18. Elkalla, E.; Khizar, S.; Tarhini, M.; Lebaz, N.; Zine, N.; Jaffrezic-Renault, N.; Errachid, A.; Elaissari, A. Core-Shell Micro/Nanocapsules: From Encapsulation to Applications. *J. Microencapsul.* **2023**, *0*, 1–32, doi:10.1080/02652048.2023.2178538.
19. Hong, R.Y.; Li, J.H.; Li, H.Z.; Ding, J.; Zheng, Y.; Wei, D.G. Synthesis of Fe3O4 Nanoparticles without Inert Gas Protection Used as Precursors of Magnetic Fluids. *J. Magn. Magn. Mater.* **2008**, *320*, 1605–1614, doi:10.1016/j.jmmm.2008.01.015.
20. Elaissari, A. Magnetic Latex Particles in Nanobiotechnologies for Biomedical Diagnostic Applications: State of the Art. *Macromol. Symp.* **2009**, *281*, 14–19, doi:10.1002/masy.200950702.
21. Anderson, E.M.; Collip, J.B. Preparation and Properties of an Antithyrotropic Substance. *Lancet* **1934**, *223*, 784–786, doi:10.1016/S0140-6736(00)92887-3.
22. Bitar, A.; Vega-Chacón, J.; Lgourna, Z.; Fessi, H.; Jafelicci, M.; Elaissari, A. Submicron Silica Shell–Magnetic Core Preparation and Characterization. *Colloids Surfaces A Physicochem. Eng. Asp.* **2018**, *537*, 318–324, doi:10.1016/j.colsurfa.2017.10.034.
23. Khizar, S.; Ahmad, N.M.; Zine, N.; Jaffrezic-Renault, N.; Errachid-El-Salhi, A.; Elaissari, A. Magnetic Nanoparticles: From Synthesis to Theranostic Applications. *ACS Appl. Nano Mater.* **2021**, *4*, 4284–4306, doi:10.1021/acsanm.1c00852.
24. Ahmed, N.; Jaafar-Maalej, C.; Eissa, M.M.; Fessi, H.; Elaissari, A. New Oil-in-Water Magnetic Emulsion as Contrast Agent for in Vivo Magnetic Resonance Imaging (MRI). *J. Biomed. Nanotechnol.* **2013**, *9*, 1579–1585, doi:10.1166/jbn.2013.1644.
25. Nagornyi, A. V.; Socoliuc, V.; Petrenko, V.I.; Almasy, L.; Ivankov, O.I.; Avdeev, M. V.; Bulavin, L.A.; Vekas, L. Structural Characterization of Concentrated Aqueous Ferrofluids. *J. Magn. Magn. Mater.* **2020**, *501*, doi:10.1016/j.jmmm.2020.166445.
26. Putra, E.G.R.; Seong, B.S.; Shin, E.; Ikram, A.; Ani, S.A.; Darminto Fractal Structures on Fe3O4 Ferrofluid: A Small-Angle Neutron Scattering Study. *J. Phys. Conf. Ser.* **2010**, *247*, doi:10.1088/1742-6596/247/1/012028.
27. Van Silfhout, A.M.; Engelkamp, H.; Erné, B.H. Colloidal Stability of Aqueous Ferrofluids at 10 T. *J. Phys. Chem. Lett.* **2020**, *11*, 5908–5912, doi:10.1021/acs.jpclett.0c01804.
28. Vékás, L.; Tombácz, E.; Turcu, R.; Morjan, I.; Avdeev, M. V.; Christoforou, T.K.; Socoliuc, V. Synthesis of Magnetic Nanoparticles and Magnetic Fluids for Biomedical Applications. *Nanomedicine - Basic Clin. Appl. Diagnostics Ther.* **2011**, *2*, 35–52, doi:10.1002/9783805598194.ch3.
29. Hong, R.Y.; Feng, B.; Liu, G.; Wang, S.; Li, H.Z.; Ding, J.M.; Zheng, Y.; Wei, D.G. Preparation and

Characterization of Fe3O4/Polystyrene Composite Particles via Inverse Emulsion Polymerization. *J. Alloys Compd.* **2009**, *476*, 612–618, doi:10.1016/j.jallcom.2008.09.060.

30. Beković, M.; Trbušić, M.; Gyergyek, S.; Trlep, M.; Jesenik, M.; Szabo, P.S.B.; Hamler, A. Numerical Model for Determining the Magnetic Loss of Magnetic Fluids. *Materials (Basel).* **2019**, *12*, doi:10.3390/ma12040591.
31. Montagne, F.; Mondain-Monval, O.; Pichot, C.; Mozzanega, H.; Elassari, A. Preparation and Characterization of Narrow Sized (o/w) Magnetic Emulsion. *J. Magn. Magn. Mater.* **2002**, *250*, 302–312, doi:10.1016/S0304-8853(02)00412-2.
32. Quy, D. Van; Hieu, N.M.; Tra, P.T.; Nam, N.H.; Hai, N.H.; Thai Son, N.; Nghia, P.T.; Anh, N.T. Van; Hong, T.T.; Luong, N.H. Synthesis of Silica-Coated Magnetic Nanoparticles and Application in the Detection of Pathogenic Viruses. *J. Nanomater.* **2013**, *2013*, doi:10.1155/2013/603940.
33. Shao, D.; Lu, M. meng; Zhao, Y. wei; Zhang, F.; Tan, Y. fei; Zheng, X.; Pan, Y.; Xiao, X. ang; Wang, Z.; Dong, W. fei; et al. The Shape Effect of Magnetic Mesoporous Silica Nanoparticles on Endocytosis, Biocompatibility and Biodistribution. *Acta Biomater.* **2017**, *49*, 531–540, doi:10.1016/j.actbio.2016.11.007.
34. Chekalil, N.; Tarhini, M.; Elaissari, A.; Saïdi-Besbes, S. Multi-Step Synthesis of Core–Shell Magnetic Nanoparticles Bearing Acid-Chelating Functional Moieties. *Res. Chem. Intermed.* **2019**, *45*, 4847–4861, doi:10.1007/s11164-019-03868-3.
35. Rosenholm, J.M.; Zhang, J.; Sun, W.; Gu, H. Large-Pore Mesoporous Silica-Coated Magnetite Core-Shell Nanocomposites and Their Relevance for Biomedical Applications. *Microporous Mesoporous Mater.* **2011**, *145*, 14–20, doi:10.1016/j.micromeso.2011.04.022.
36. Ebadi, M.; Bullo, S.; Buskara, K.; Hussein, M.Z.; Fakurazi, S.; Pastorin, G. Release of a Liver Anticancer Drug, Sorafenib from Its PVA/LDH- and PEG/LDH-Coated Iron Oxide Nanoparticles for Drug Delivery Applications. *Sci. Rep.* **2020**, *10*, 1–19, doi:10.1038/s41598-020-76504-5.
37. Song, R.; Zhang, M.; Liu, Y.; Cui, Z.; Zhang, H.; Tang, Z.; Chen, X.; Wu, H.; Yao, Z.; He, M.; et al. A Multifunctional Nanotheranostic for the Intelligent MRI Diagnosis and Synergistic Treatment of Hypoxic Tumor. *Biomaterials* **2018**, *175*, 123–133, doi:10.1016/j.biomaterials.2018.05.018.
38. Matsumura, S.; Hlil, A.R.; Lepiller, C.; Gaudet, J.; Guay, D.; Shi, Z.; Holdcroft, S.; Hay, A.S. Stability and Utility of Pyridyl Disulfide Functionality in RAFT and Conventional Radical Polymerizations. *J. Polym. Sci. Part A Polym. Chem.* **2008**, *46*, 7207–7224, doi:10.1002/pola.
39. Rahman, M.M.; Montagne, F.; Fessi, H.; Elaissari, A. Anisotropic Magnetic Microparticles from Ferrofluid Emulsion. *Soft Matter* **2011**, *7*, 1483–1490, doi:10.1039/c0sm00602e.
40. Ahmed, N.; Ahmad, N.M.; Fessi, H.; Elaissari, A. In Vitro MRI of Biodegradable Hybrid (Iron Oxide/Polycaprolactone) Magnetic Nanoparticles Prepared via Modified Double Emulsion Evaporation Mechanism. *Colloids Surfaces B Biointerfaces* **2015**, *130*, 264–271, doi:10.1016/j.colsurfb.2015.04.022.
41. Tasmia; Shah, J.; Jan, M.R. Microextraction of Selected Endocrine Disrupting Phenolic Compounds Using Magnetic Chitosan Biopolymer Graphene Oxide Nanocomposite. *J. Polym. Environ.* **2020**, *28*, 1673–1683, doi:10.1007/s10924-020-01714-x.
42. Elizondo-Villarreal, N.; Verástegui-Domínguez, L.; Rodríguez-Batista, R.; Gándara-Martínez, E.; Alcorta-García, A.; Martínez-Delgado, D.; Rodríguez-Castellanos, E.A.; Vázquez-Rodríguez, F.; Gómez-Rodríguez, C. Green Synthesis of Magnetic Nanoparticles of Iron Oxide Using Aqueous Extracts of Lemon Peel Waste and Its

Application in Anti-Corrosive Coatings. *Materials (Basel).* **2022**, *15*, doi:10.3390/ma15238328.

43. Asab, G.; Zereffa, E.A.; Abdo Seghne, T. Synthesis of Silica-Coated Fe3O4 Nanoparticles by Microemulsion Method: Characterization and Evaluation of Antimicrobial Activity. *Int. J. Biomater.* **2020**, *2020*, doi:10.1155/2020/4783612.
44. Lun, H.; Ouyang, J.; Yang, H. Enhancing Dispersion of Halloysite Nanotubes via Chemical Modification. *Phys. Chem. Miner.* **2014**, *41*, 281–288, doi:10.1007/s00269-013-0646-9.
45. Ibrahim, I.; Belessiotis, G. V.; Arfanis, M.K.; Athanasekou, C.; Philippopoulos, A.I.; Mitsopoulou, C.A.; Romanos, G.E.; Falaras, P. Surfactant Effects on the Synthesis of Redox Bifunctional V2o5 Photocatalysts. *Materials (Basel).* **2020**, *13*, 1–13, doi:10.3390/ma13204665.
46. Islam, M.N.; Abbas, M.; Sinha, B.; Joeng, J.R.; Kim, C.G. Silica Encapsulation of Sonochemically Synthesized Iron Oxide Nanoparticles. *Electron. Mater. Lett.* **2013**, *9*, 817–820, doi:10.1007/s13391-013-6019-1.
47. Adhikary, S.K.; Rudžionis, Ž.; Tučkutė, S.; Ashish, D.K. Effects of Carbon Nanotubes on Expanded Glass and Silica Aerogel Based Lightweight Concrete. *Sci. Rep.* **2021**, *11*, 1–11, doi:10.1038/s41598-021-81665-y.
48. Sjögren-Levin, E.; Pantleon, W.; Ahadi, A.; Hegedüs, Z.; Lienert, U.; Tsuji, N.; Ameyama, K.; Orlov, D. Separation of XRD Peak Profiles in Single-Phase Metals with Bimodal Grain Structure to Analyze Stress Partitioning. *IOP Conf. Ser. Mater. Sci. Eng.* **2022**, *1249*, 012040, doi:10.1088/1757-899x/1249/1/012040.
49. Ahmadi, A.; Ramezanzadeh, B.; Mahdavian, M. *Hybrid Silane Coating Reinforced with Silanized Graphene Oxide Nanosheets with Improved Corrosion Protective Performance*; 2016; Vol. 6; ISBN 9821229697.
50. Shen, H.; Chen, W.; Li, J.; Li, X.; Yang, H. Biofunctional Magnetic Nanoparticles as a General Agent to Immobilize Proteins Contained in Traditional Chinese Medicines. *Microchim. Acta* **2007**, *157*, 49–54, doi:10.1007/s00604-006-0648-0.
51. Foroozan, E.A.; Naderi, R. Effect of Coating Composition on the Anticorrosion Performance of a Silane Sol-Gel Layer on Mild Steel. *RSC Adv.* **2015**, *5*, 106485–106491, doi:10.1039/c5ra21744j.
52. Sahoo, Y.; Goodarzi, A.; Swihart, M.T.; Ohulchanskyy, T.Y.; Kaur, N.; Furlani, E.P.; Prasad, P.N. Aqueous Ferrofluid of Magnetite Nanoparticles: Fluorescence Labeling and Magnetophoretic Control. *J. Phys. Chem. B* **2005**, *109*, 3879–3885, doi:10.1021/jp045402y.
53. Ashraf, M.A.; Liu, Z.; Peng, W.X. Trisaminomethane–Cobalt Complex Supported on Fe3O4 Magnetic Nanoparticles as an Efficient Recoverable Nanocatalyst for Oxidation of Sulfides and C–S Coupling Reactions. *Appl. Organomet. Chem.* **2020**, *34*, 1–15, doi:10.1002/aoc.5260.
54. Liu, T.Y.; Hu, S.H.; Hu, S.H.; Tsai, S.P.; Chen, S.Y. Preparation and Characterization of Thermal-Sensitive Ferrofluids for Drug Delivery Application. *J. Magn. Magn. Mater.* **2007**, *310*, 2850–2852, doi:10.1016/j.jmmm.2006.11.129.
55. Gemeay, A.H.; Keshta, B.E.; El-Sharkawy, R.G.; Zaki, A.B. Chemical Insight into the Adsorption of Reactive Wool Dyes onto Amine-Functionalized Magnetite/Silica Core-Shell from Industrial Wastewaters. *Environ. Sci. Pollut. Res.* **2020**, *27*, 32341–32358, doi:10.1007/s11356-019-06530-y.